

$(d, {}^3\text{He})$ reaction on odd-neutron nuclear target for the formation of deeply bound pionic atoms

Natsumi Ikeno^{1,*}, Junko Yamagata-Sekihara^{2,3} Hideko Nagahiro¹, and Satoru Hirenzaki¹

¹*Department of Physics, Nara Women's University, Nara 630-8506, Japan*

²*Research Center for Physics and Mathematics, Osaka Electro-Communication University, Neyagawa, Osaka 572-8530, Japan*

³*Institute of Particle and Nuclear Studies, High Energy Accelerator Research Organization (KEK), 1-1, Oho, Ibaraki 305-0801, Japan*

**E-mail: jan_ikeno@cc.nara-wu.ac.jp*

.....
We consider the pionic atom spectroscopy by the $(d, {}^3\text{He})$ reaction on an odd-neutron nuclear target in this article, which has not been investigated so far. In the $(d, {}^3\text{He})$ reaction on the odd-neutron nuclear target, we can observe the pionic states in the even-neutron nucleus with spin-parity 0^+ . We expect that this pionic state does not have the additional shifts due to the effects of the residual interaction between neutron-hole and pionic states. For the even-neutron nuclear target cases, we may have to take into account the residual interaction effects to deduce the binding energies of the pionic states precisely from the high precision experimental data since the final pionic states are the pion-particle plus neutron-hole $[\pi \otimes n^{-1}]$ states. Thus, in addition to widening the domain of the pionic atom spectroscopy in nuclear chart, the present study of the $(d, {}^3\text{He})$ reaction on the odd-neutron target is considered to be important to deduce extremely precise information on the binding energies of the observed pionic states, and to know the pion properties and aspects of the symmetries of the strong interaction at finite density.

We modify the formula of the even-even nuclear target case to study the pionic atom formation spectra on the even-odd nuclear target and show the numerical results of ${}^{117}\text{Sn}$ target case. This experiment will be performed at RIBF/RIKEN in near future.

.....
Subject Index D15,D33,D25,D22

1. Introduction

One of the most interesting subjects in the contemporary hadron-nuclear physics is to study the aspects of the QCD symmetry in the extreme conditions with high density and/or temperature [1]. To know the hadron properties in these extreme conditions is an important way to find the consequences of the change of the symmetry breaking pattern of QCD based on the deep understanding of the origin of the hadron properties such as their masses and interactions [2].

Meson-nucleus systems are very interesting objects in this context to deduce the hadron properties at finite density [3, 4]. In Ref. [5], the partial restoration of chiral symmetry is concluded by determining the pion weak decay constant f_π from the observation of deeply bound pionic atoms using the Tomozawa–Weinberg and Gell-Mann–Oakes–Renner relations. The theoretical foundation of this scenario is strengthened by Refs. [6, 7]. The effects

of $U_A(1)$ anomaly at finite density is also discussed in Refs. [8–12] with the possible existence and observation of the $\eta'(958)$ mesic nucleus. Kaonic [13–17] and η [18–22] mesic nucleus systems are also interesting because of the existence of the resonances, $\Lambda(1405)$ and $N^*(1535)$, which are strongly coupled to $\bar{K}N$ and ηN channels, respectively.

Within these meson-nucleus systems, the pionic atom is the best system to perform accurate spectroscopic studies at present since we have the well-established theoretical and experimental techniques. So far, based on the theoretical predictions [23–27], there exist in the world four sets of the successful experimental results for the formation of the deeply bound pionic atoms in the $(d, {}^3\text{He})$ reaction [5, 28–32]. However, all theoretical and experimental efforts concentrated on the even-even nuclear target cases.

In this article, we report a theoretical study of the deeply bound pionic atom formation in the $(d, {}^3\text{He})$ reaction on the odd-neutron (odd-N) nuclear target ${}^{117}\text{Sn}$. The reasons why we consider the odd-N nuclear target cases are followings.

In the $(d, {}^3\text{He})$ reaction for the pionic atom formation on an even-neutron nuclear target, one neutron in the target nucleus is picked-up and removed from the nucleus. Consequently, there exists a neutron-hole state j_n^{-1} in the daughter nucleus which couples to pionic atom states $(n_\pi \ell_\pi)$ to make total spin J state $[j_n^{-1} \otimes \ell_\pi]_J$. In these states, we generally expect the existence of the residual interaction effects and of the level splittings between different J states [33, 34]. The experimental errors of the pion binding energies and widths reported in Ref. [5] are approaching the magnitude of the estimated level shifts and width changes due to the residual interaction [33, 34]. Thus, the formation of the pionic states on the even-even nucleus by the $(d, {}^3\text{He})$ reactions on the odd-N nuclear target is preferable to avoid the additional difficulties due to the residual interaction effects to determine the pion binding energies precisely and to extract the most accurate information on the parameter of the QCD symmetry from the observation. Actually, in Ref. [35], Ikeno *et al.* reported that we need very accurate spectroscopic studies of the pionic atoms to deduce the density dependence of the chiral condensate $\langle \bar{q}q \rangle$ from the observation beyond the linear density approximation [36]. It is also interesting and important to widen the domain of the spectroscopic studies of the deeply bound pionic states by including the odd-N target for the systematic information on pion-nucleus systems and the study of the reaction mechanism of the pionic atom formation as in the case of analyzing the reaction at finite angles [37].

In this article, we report the theoretical study of the $(d, {}^3\text{He})$ reaction for the pionic atom formation on the odd-N nuclear targets ${}^{117}\text{Sn}$.

2. Effective Number Approach

In the effective number approach in this article, we assume the neutron configuration of the ground state of the target nucleus as,

$$|i\rangle = |s_{1/2} \otimes 0^+\rangle, \quad (1)$$

by considering the odd-N nucleus with $J^P = \frac{1}{2}^+$ such as ${}^{117}\text{Sn}$ and ${}^{119}\text{Sn}$. In Eq. (1), we consider an extra neutron exists in the $s_{1/2}$ orbit together with the $J^P = 0^+$ even-even core nucleus in the target. As for the final state, we distinguish two cases in our formula which are written as,

$$|f\rangle = \begin{cases} |\ell_\pi \otimes 0^+\rangle \\ |(\ell_\pi \otimes [s_{1/2} \otimes j_h^{-1}]_J)_{J_f}\rangle \end{cases}, \quad (2)$$

where we write the quantum number of the extra neutron state as $s_{1/2}$ and the neutron hole state as j_h^{-1} with the total angular momentum J of the daughter nucleus. The angular momentum of the pion bound state is written as ℓ_π and the total angular momentum of the pionic atom as J_f . In the first line in Eq. (2), we consider the final state with the atomic pion and the even-even core nucleus in the ground state after the extra $s_{1/2}$ neutron is removed from the target in the ($d, {}^3\text{He}$) reaction. In the second line in Eq. (2), one neutron is considered to be picked-up from other neutron state leaving a neutron-hole j_h^{-1} in the core of the daughter nucleus.

The contributions of these final states to the ($d, {}^3\text{He}$) spectra are evaluated as the effective numbers $N_{\text{eff}}^{(1)}$ and $N_{\text{eff}}^{(2)}$ defined by,

$$N_{\text{eff}}^{(1)} = \frac{1}{2} \sum_{m_n} \sum_{m_\pi} \sum_{m_s} \left| \int d\mathbf{r} e^{i\mathbf{q}\cdot\mathbf{r}} D(\mathbf{r}) \xi_{\frac{1}{2}m_s}^\dagger \langle \ell_\pi \otimes 0^+ | \hat{\phi}_\pi^\dagger(\mathbf{r}) \hat{\psi}_n(\mathbf{r}) | s_{1/2} \otimes 0^+ \rangle \right|^2, \quad (3)$$

and

$$N_{\text{eff}}^{(2)} = \frac{1}{2} \sum_{m_n} \sum_{J_f M_f} \sum_{m_s} \left| \int d\mathbf{r} e^{i\mathbf{q}\cdot\mathbf{r}} D(\mathbf{r}) \xi_{\frac{1}{2}m_s}^\dagger \langle (\ell_\pi \otimes [s_{1/2} \otimes j_h^{-1}]_J)_{J_f} | \hat{\phi}_\pi^\dagger(\mathbf{r}) \hat{\psi}_n(\mathbf{r}) | s_{1/2} \otimes 0^+ \rangle \right|^2. \quad (4)$$

$N_{\text{eff}}^{(1)}$ is the effective number for the pionic atom formation in the case of neutron pick-up from the $s_{1/2}$ orbit in the target nucleus and $N_{\text{eff}}^{(2)}$ is that of neutron pick-up from a single particle orbit j_h other than $s_{1/2}$, which corresponds to the final states shown in Eq. (2). $\hat{\phi}_\pi^\dagger$ and $\hat{\psi}_n$ indicate the field operators of pion and neutron in analogous with the formula for the even-even nuclear target [25, 26]. The spin wave function of the picked-up neutron is denoted as $\xi_{\frac{1}{2}m_s}$, and we take the spin average with respect to m_s so as to take into account the possible spin direction of the neutrons in the target nucleus. We take the spin average of the neutron in the $s_{1/2}$ state in the target as indicated by $\frac{1}{2} \sum_{m_n}$ in Eqs. (3) and (4). We use the Eikonal approximation and write the projectile (d) distorted wave χ_d and the ejectile (${}^3\text{He}$) distorted wave χ_{He}^* as,

$$\chi_{\text{He}}^*(\mathbf{r}) \chi_d(\mathbf{r}) = e^{i\mathbf{q}\cdot\mathbf{r}} D(\mathbf{r}), \quad (5)$$

where \mathbf{q} is the momentum transfer between the projectile and the ejectile, and the distortion factor $D(\mathbf{r})$ is defined as

$$D(\mathbf{r}) = D(z, \mathbf{b}) = \exp \left[-\frac{1}{2} \sigma_{dN} \int_{-\infty}^z dz' \rho_A(z', \mathbf{b}) - \frac{1}{2} \sigma_{hN} \int_z^{\infty} dz' \rho_{A-1}(z', \mathbf{b}) \right]. \quad (6)$$

Here, the deuteron-nucleon and ${}^3\text{He}$ -nucleon total cross sections are denoted as σ_{dN} and σ_{hN} . The function $\rho_A(z, \mathbf{b})$ and $\rho_{A-1}(z, \mathbf{b})$ are the density distributions of the target and daughter nuclei at beam-direction coordinate z with impact parameter \mathbf{b} .

The effective numbers $N_{\text{eff}}^{(1)}$ and $N_{\text{eff}}^{(2)}$ in Eqs. (3) and (4) are manipulated separately and they are reduced to

$$N_{\text{eff}}^{(1)} = \sum_{m_\pi} \left| \int d\mathbf{r} e^{i\mathbf{q}\cdot\mathbf{r}} D(\mathbf{r}) \phi_{\ell_\pi m_\pi}^*(\mathbf{r}) \phi_{00}(\mathbf{r}) \right|^2, \quad (7)$$

and

$$\begin{aligned}
N_{\text{eff}}^{(2)} &= \frac{1}{2} \sum_{J_f j} \sum_{\ell n} \left| \langle 6j \rangle \langle 6j' \rangle \sqrt{\frac{2J_f + 1}{2\ell + 1}} \sum_{m_\pi m_h} (\ell_\pi m_\pi \ell_h m_h | \ell n) (-)^{\ell_h - m_h} \right. \\
&\quad \times \left. \int d\mathbf{r} e^{i\mathbf{q} \cdot \mathbf{r}} D(\mathbf{r}) \phi_{\ell_\pi m_\pi}^*(\mathbf{r}) \phi_{\ell_h - m_h}(\mathbf{r}) \right|^2, \tag{8}
\end{aligned}$$

respectively. Here, $\phi_{\ell_\pi m_\pi}$ indicates the spatial wave function of the pion in the daughter nucleus and $\phi_{\ell_h m_h}$ that of the neutron bound state in the target nucleus. The pion wave function $\phi_{\ell_\pi m_\pi}$ is calculated by solving the Klein-Gordon equation with the realistic potential including the finite Coulomb potential and the optical potential [4]. For the neutron, we use the calculated spatial wave function $\phi_{\ell_h m_h}$ by the neutron potential reported in Ref. [38].

In Eq. (8), the $\langle 6j \rangle$ symbol indicates the coefficient of the expansion as

$$\begin{aligned}
\langle 6j \rangle &= \langle (\ell_\pi j_h) j s_{1/2}; J_f | \ell_\pi (j_h s_{1/2}) J; J_f \rangle \\
&= \sqrt{(2j + 1)(2J + 1)} W(\ell_\pi j_h J_f \frac{1}{2}; j J) \\
&= \sqrt{(2j + 1)(2J + 1)} (-)^{-(\ell_\pi + j_h + J_f + \frac{1}{2})} \left\{ \begin{array}{ccc} \ell_\pi & j_h & j \\ \frac{1}{2} & J_f & J \end{array} \right\}, \tag{9}
\end{aligned}$$

where $W(\ell_\pi j_h J_f \frac{1}{2}; j J)$ is the Racah coefficient and $\left\{ \begin{array}{ccc} \ell_\pi & j_h & j \\ \frac{1}{2} & J_f & J \end{array} \right\}$ the $6j$ -symbol. The symbol $\langle 6j' \rangle$ also indicates the coefficient of the expansion $\langle (\ell_\pi \ell_h) \ell \frac{1}{2}; j | \ell_\pi (\ell_h \frac{1}{2}) j_h; j \rangle$.

Using these effective numbers, the bound state formation cross section can be written as,

$$\left(\frac{d^2\sigma}{dE_{\text{He}} d\Omega_{\text{He}}} \right)_A^{\text{lab}} = \left(\frac{d\sigma}{d\Omega_{\text{He}}} \right)_{\text{ele}}^{\text{lab}} \sum_{i=1}^2 \sum_{\text{spins}} K \frac{\Gamma}{2\pi} \frac{1}{\Delta E^2 + \Gamma^2/4} N_{\text{eff}}^{(i)}, \tag{10}$$

where the symbol of the sum of spin quantum numbers \sum_{spins} indicates \sum_{ℓ_π} for $i = 1$ and $\sum_{\ell_\pi j_h J}$ for $i = 2$, respectively.

Here, $\left(\frac{d\sigma}{d\Omega_{\text{He}}} \right)_{\text{ele}}^{\text{lab}}$ indicates the elementary differential cross section for the $d + n \rightarrow {}^3\text{He} + \pi^-$ reaction in the laboratory system, which is extracted from the experimental data [39] of the $p + d \rightarrow t + \pi^+$ reaction assuming charge symmetry [37]. We use the Lorentz distribution function $\frac{\Gamma}{2\pi} \frac{1}{\Delta E^2 + \Gamma^2/4}$ to account for the width Γ of the pion bound state, where ΔE is defined as $\Delta E = E_{\text{He}} + E_\pi - E_d - E_n$. E_n is the energy of neutron in the target nucleus and defined as $E_n = M_n - S_n(j_n)$ with the neutron separation energy S_n from the j_n single particle level and the neutron mass M_n . E_π is the energy of the pion bound state defined as $E_\pi = m_\pi - B.E.(\ell_\pi)$ with the pion mass m_π and the binding energy $B.E.$ of the bound state indicated by ℓ_π . The reaction Q -value can be expressed as $Q = \Delta E - m_\pi + B.E.(\ell_\pi) - S_n(j_n) + (M_n + M_d - M_{\text{He}})$, where $M_n + M_d - M_{\text{He}} = 6.787$ MeV.

The kinematical correction factor K in Eq. (10) is defined as

$$K = \left[\frac{|\mathbf{p}_{\text{He}}^A|}{|\mathbf{p}_{\text{He}}|} \frac{E_n E_\pi}{E_n^A E_\pi^A} \left(1 + \frac{E_{\text{He}}}{E_\pi} \frac{|\mathbf{p}_{\text{He}}| - |\mathbf{p}_d| \cos\theta_{d\text{He}}}{|\mathbf{p}_{\text{He}}|} \right) \right]^{\text{lab}}, \tag{11}$$

where the superscript ‘A’ indicates the momentum and energy which are evaluated in the kinematics of the nuclear target case [37]. The superscript ‘lab’ indicates that all kinematical variables are evaluated in the laboratory frame. This correction factor is $K = 1$ for the recoilless kinematics at $\theta_{d\text{He}}^{\text{lab}} = 0^\circ$ with $S_n = 0$ and $B.E. = 0$.

As for the quasi-free contributions, we can express the cross section as,

$$\left(\frac{d^2\sigma}{dE_{\text{He}}d\Omega_{\text{He}}}\right)_A^{\text{lab}} = \left(\frac{d\sigma}{d\Omega_{\text{He}}}\right)_{\text{ele}}^{\text{lab}} \sum_{i=1}^2 \sum_{\text{spins}} \frac{2|\mathbf{p}_\pi^A|E_\pi^A}{\pi} KN_{\text{eff}}^{(i)}. \quad (12)$$

The definition of the symbol \sum_{spins} is the same as in Eq. (10). The factor $\frac{2|\mathbf{p}_\pi^A|E_\pi^A}{\pi}$ is due to the phase volume of the unbound pion [40].

In order to predict the realistic spectrum shape of the $(d, {}^3\text{He})$ reactions for the pionic state formation, we need to take into account the realistic ground-state configurations of the target nuclei, the nuclear excitation energies, and the relative excitation strengths leading to the excited states of the daughter nuclei. First, we need to normalize the calculated effective numbers using the neutron occupation probability of each single particle state in the ground state of the target nucleus to obtain a realistic total strength for the neutron pick-up process from each orbital. The occupation probabilities are obtained from the analyses of the data of the one neutron pick-up reactions such as (p, d) and (d, t) and are not equal to one in general.

As for the excited levels of the daughter nuclei, we use the experimental excitation energies and strengths obtained from the one neutron pick-up reactions. For odd-N nuclear target case with $J^P = \frac{1}{2}^+$ such as ${}^{117}\text{Sn}$, we consider two kinds of the final state separately as shown in Eq. (2). If a single neutron is picked-up from the neutron orbit $s_{1/2}$ in the target, the daughter nucleus is expected to have total angular momentum $J^P = 0^+$. In our formula, the effective number $N_{\text{eff}}^{(1)}$ for the pionic state (ℓ_π) formation with such a state is modified as,

$$N_{\text{eff}}^{(1)} \rightarrow N_{\text{eff}}^{(1)}(\ell_\pi \otimes (J^P = 0^+)) \times F_O(s_{1/2}) \times \begin{cases} F_R((J^P = 0^+)_1), \\ F_R((J^P = 0^+)_2), \\ \dots \\ F_R((J^P = 0^+)_N), \end{cases} \quad (13)$$

where ‘N’ indicates the number of states of the daughter nucleus with $J^P = 0^+$. And $N_{\text{eff}}^{(1)}(\ell_\pi \otimes (J^P = 0^+))$ is the effective number defined in Eq. (3), F_O the normalization factor due to the occupation probabilities of the neutron states $s_{1/2}$ in the target nucleus, and F_R the relative strength factor of the N -th excited state in the daughter nucleus with total angular momentum $J^P = 0^+$ [27, 41]. The contributions from the all $J^P = 0^+$ nuclear excited states are obtained by summing up the r.h.s of Eq. (10) with the realistic (experimental) excitation energies which appeared in ΔE .

Then, if a single neutron is picked-up from other neutron orbit j_h , the daughter nucleus has the total angular momentum $J = [s_{1/2} \otimes j_h^{-1}]$. The effective number $N_{\text{eff}}^{(2)}$ for the pionic state (ℓ_π) formation with the excited state of the daughter nucleus with $J = [s_{1/2} \otimes j_h^{-1}]$ is

modified in our model as,

$$N_{\text{eff}}^{(2)} \rightarrow N_{\text{eff}}^{(2)}(\ell_{\pi} \otimes [s_{1/2} \otimes j_h^{-1}]_J) \times F_O(j_h) \times \begin{cases} F_R([s_{1/2} \otimes j_h^{-1}]_J)_1, \\ F_R([s_{1/2} \otimes j_h^{-1}]_J)_2, \\ \dots \\ F_R([s_{1/2} \otimes j_h^{-1}]_J)_N, \end{cases} \quad (14)$$

where ‘ N ’ indicates the number of states of the daughter nucleus with spin J . And $N_{\text{eff}}^{(2)}(\ell_{\pi} \otimes [s_{1/2} \otimes j_h^{-1}]_J)$ is the effective number defined in Eq. (4), F_O the normalization factor due to the occupation probabilities of the neutron states j_h in the target nucleus, and F_R the relative strength factor of the N -th excited states in the daughter nucleus with total angular momentum J with a j_h^{-1} neutron hole [27, 41]. The contributions from all the nuclear excited states with total angular momentum J are obtained by summing up them in Eq. (10) as in the case with $J^P = 0^+$ described above.

We show in the next section the concrete examples of the application of the F_O and F_R obtained from the $^{117}\text{Sn}(d, t)^{116}\text{Sn}$ reaction [42] to calculate the spectra of the $^{117}\text{Sn}(d, ^3\text{He})$ reactions for the pionic atom formation.

3. Numerical Result

We show the calculated results of the $^{117}\text{Sn}(d, ^3\text{He})$ reaction spectra for the formation of the deeply bound pionic states in ^{116}Sn , and compare the spectra with that of the ^{122}Sn nuclear target case. We determine firstly the normalization factors F_O of the neutron states in the target nucleus and the relative strengths F_R of the nuclear excited levels of the daughter nucleus using the spectroscopic strength obtained from $^{117}\text{Sn}(d, t)^{116}\text{Sn}$ data [42].

In the Table 2 of Ref. [42], we can find the compilation of the data of the excitation energy E_x , the spin-parity J^P of the final nuclear state, and the spectroscopic strength $G(j_h)$ of the the neutron hole state j_h . As we can see from the table, the quantum numbers of the some of the excited states could not be determined by the analyses of the experiment in Ref. [42]. The spin-parity J^P is missing for the levels of $E_x = 3.228, 3.315, 3.371, 3.470, 3.513, 3.589, 3.618, 3.772, 3.950, 4.037, 4.084$ MeV, and the spectroscopic strength $G(j_h)$ of the neutron hole state is not uniquely determined for $J^P = 2^+$ states which are written as $G(d_{3/2}$ or $d_{5/2})$ in the table. The spin-parity is not uniquely determined for the level of $E_x = 3.739$ MeV.

In order to make use of these data [42] to determine the F_O and F_R factors, we need to make a few assumptions to compensate for the missing information in the Table 2 of Ref. [42]. First, we assume the value of the missing and not-uniquely determined ($E_x = 3.739$ MeV) spin-parity of the states listed in the column of $G(d_{3/2}$ or $d_{5/2})$ to be $J^P = 2^+$ since it can be realized for both $d_{3/2}$ and $d_{5/2}$ states by coupling to the $s_{1/2}$ state. Then, we assume that the spectroscopic strength of the levels, for which the observed strengths are written in the *both* columns of $d_{3/2}$ and $d_{5/2}$ of $G(d_{3/2}$ or $d_{5/2})$, is equally shared by the contributions for $j_h = d_{3/2}$ and $d_{5/2}$ states. For example, the spectroscopic strength $G(d_{3/2}$ or $d_{5/2})$ at $E_x = 1.294$ MeV is written as $G(d_{3/2}) = 0.20$ and $G(d_{5/2}) = 0.16$ in Table 2 in Ref. [42]. This means that the observed strength corresponds to $G = 0.20$ in case of $j_h = d_{3/2}$, and $G = 0.16$ for $j_h = d_{5/2}$ case. We assume that there exist the half contributions from both j_h as $G(d_{3/2}) = 0.10$ and $G(d_{5/2}) = 0.08$. We determine all spectroscopic strength $G(d_{3/2})$ and $G(d_{5/2})$ in a similar way. We also assume that the spin-parity of the level at $E_x = 3.315$

Table 1 Compilation of the normalization factor (F_O) corresponding to the occupation probability of each neutron state in the ground state of ^{117}Sn determined from the experimental data in Ref. [42]. See details in the text.

Neutron hole orbit (j_h)	Normalization factor (F_O)
$3s_{1/2}$	0.47
$2d_{3/2}$	0.40
$2d_{5/2}$	0.39
$1g_{7/2}$	0.80
$1h_{11/2}$	0.11

MeV is $J^P = 3^+$. Since the strength of this level is small, this assumption will not affect the final results. Finally, we neglect the level of $f_{5/2}$ or $f_{7/2}$ in $E_x = 2.266$ MeV in Table 2 of Ref. [42] since the strength of these excitations is small and they correspond to the core polarization effects in the naive shell model.

Based on the assumptions described above, we use the data in Ref. [42] to determine the F_O and F_R factors. In Table 1, we summarize the normalization factors F_O corresponding to the occupation probabilities of the neutron orbit j_h in the target ^{117}Sn . Since the sum of the spectroscopic strength $G(j_h)$ in Ref. [42] is expected to be equal to the number of the neutron in the neutron orbit (j_h) in the target, we evaluate $F_O(j_h)$ as,

$$F_O(j_h) = \frac{1}{(2j_h + 1)} \sum_N G(j_h)_N, \quad (15)$$

where $G(j_h)_N$ indicates the spectroscopic strength of the N -th nuclear levels with a hole state j_h in the daughter nucleus. As for $j_h = s_{1/2}$ case, we evaluate $F_O(s_{1/2})$ as,

$$F_O(s_{1/2}) = \sum_N G(s_{1/2})_N, \quad (16)$$

since we assumed that the number of the neutron in the $s_{1/2}$ orbit in the odd- N target nucleus with $J^P = \frac{1}{2}^+$ is equal to be 1 for fully occupied case as shown in Eq. (1) in the effective number formalism in Section 2.

In Table 2, we summarize the spin-parity J^P , the excitation energies E_x , the neutron hole orbit j_h , and the relative strength F_R of the excited states of ^{116}Sn determined from the data of $^{117}\text{Sn}(d, t)^{116}\text{Sn}$ in Ref. [42] with some assumptions described before. We determine the relative strength F_R using the spectroscopic strength $G(j_h)$ in Ref. [42] again. We evaluate $F_R([s_{1/2} \otimes j_h^{-1}]_J)_N$ as,

$$F_R([s_{1/2} \otimes j_h^{-1}]_J)_N = \frac{G(j_h)_{N,J}}{\sum_N G(j_h)_{N,J}}, \quad (17)$$

where $G(j_h)_{N,J}$ indicates the spectroscopic strength of the N -th nuclear levels with a hole state j_h and total spin J in the daughter nucleus. For $j_h = s_{1/2}$ case, we evaluate $F_R((J^P = 0^+)_N)$ as,

$$F_R((J^P = 0^+)_N) = \frac{G(s_{1/2})_{N,0^+}}{\sum_N G(s_{1/2})_{N,0^+}}. \quad (18)$$

Table 2 Excitation energy (E_x) and relative strength (F_R) of each excited level in ^{116}Sn determined from the experimental data of the $^{117}\text{Sn}(d,t)$ reactions [42]. See the text for details.

J^P	E_x [MeV]	Neutron hole orbit j_h	F_R	Neutron hole orbit j_h	F_R
0^+	0.000	$3s_{1/2}$	0.68		
	1.757		0.13		
	2.027		0.11		
	2.545		0.09		
1^+	2.587	$2d_{3/2}$	0.92		
	2.960		0.08		
2^+	1.294	$2d_{3/2}$	0.07	$2d_{5/2}$	0.08
	2.112		0.00		0.00
	2.225		0.09		0.09
	2.650		0.00		0.00
	2.843		0.03		0.03
	3.228		0.09		0.09
	3.371		0.09		0.09
	3.470		0.10		0.10
	3.513		0.03		0.03
	3.589		0.14		0.14
	3.618		0.01		0.01
	3.739		0.03		0.03
	3.772		0.14		0.14
	3.950		0.13		0.13
	4.037		0.03		0.03
4.084	0.02	0.02			
3^+	2.997	$2d_{5/2}$	0.05	$1g_{7/2}$	0.26
	3.180				0.43
	3.315				0.02
	3.416		0.37		0.06
	3.709		0.59		0.23
4^+	2.390	$1g_{7/2}$	0.08		
	2.529		0.09		
	2.801		0.21		
	3.046		0.15		
	3.096		0.48		
5^-	2.366	$1h_{11/2}$	1.00		
6^-	2.773	$1h_{11/2}$	1.00		

In Fig. 1, we show the calculated spectra for the pionic states formation at $\theta_{d\text{He}}^{\text{lab}} = 0^\circ$ in the $^{117}\text{Sn}(d,^3\text{He})$ and $^{122}\text{Sn}(d,^3\text{He})$ reactions. In addition to the total spectra, the contributions of the deeply bound pionic states formation, and the quasi-free π^- and π^0 production are also shown separately. The dominant subcomponents are indicated in the figure with

Table 3 Excitation energy (E_x) and relative strength (F_R) of each excited level in ^{121}In determined from the experimental data of the $^{122}\text{Sn}(d,^3\text{He})^{121}\text{In}$ reaction [43]. The normalization factor (F_O) corresponding to the occupation probability of each proton state in the ground state of ^{122}Sn is also listed. Here, we have assumed the level at $E_x = 1.40$ MeV to be $1f_{5/2}$ state, which was not identified clearly in Ref. [43].

Proton hole orbit (j_h)	E_x [MeV]	Relative strength (F_R)	Normalization factor (F_O)
$1g_{9/2}$	0.00	1.0	1.0
$2p_{1/2}$	0.31	1.0	1.0
$2p_{3/2}$	0.62	1.0	1.0
$1f_{5/2}$	1.40	1.0	1.0

their quantum numbers. In the $^{117}\text{Sn}(d,^3\text{He})$ spectra, the contributions from the final states $[(n\ell)_\pi \otimes J^P]$ with $J^P = 0^+$ and $\ell_\pi = 0$ are dominant. We find that we can see clearly the peak structure of the pionic $1s$ state formation with the ground state of the even-even nucleus ^{116}Sn as indicated in the figure as $[(1s)_\pi \otimes 0^+_{\text{ground}}]$. The subcomponents coupled to the ground state of the daughter nucleus ^{116}Sn in the upper figure of Fig. 1 will not have the additional shifts due to the residual interaction effects. In the $^{122}\text{Sn}(d,^3\text{He})$ spectra (lower figure), the cross section in the bound pion region is the same as in Ref. [37].

In both $^{117}\text{Sn}(d,^3\text{He})$ and $^{122}\text{Sn}(d,^3\text{He})$ spectra, the contribution from the pionic $1s$ state formation with the neutron s hole state is found to be large because of the matching condition with the recoilless kinematics. We find that the total spectrum of the bound pionic state formation in $^{117}\text{Sn}(d,^3\text{He})$ reaction spreads into wider energy range than that in $^{122}\text{Sn}(d,^3\text{He})$ reaction. This is because the excited levels of ^{116}Sn tend to have larger excitation energies (E_x) than those of ^{121}Sn [35].

As shown in Fig. 1, the π^0 quasi-free production contribution is found to be much smaller than that of π^- . Here, the contribution of the quasi-free π^0 production in the $^{117}\text{Sn}(d,^3\text{He})$ spectra is estimated approximately as explained below.

To calculate the contributions of the quasi-free π^0 production, we use the experimental data of the single proton pick-up reactions from the same target to determine the excitation energies and strengths of the one proton-hole states of the nucleus as in the case of π^- production with a neutron-hole. In the ^{117}Sn target case, we do not find the appropriate experimental data of the single proton pick-up reactions. Therefore, as the quasi-free π^0 production contributions of the ^{117}Sn target case, we assume the same as those of the ^{122}Sn target except the shift of the threshold energy. We consider that this assumption does not affect the essential structure of the total spectrum since the contribution of the quasi-free π^0 production is much smaller than that of the quasi-free π^- production around the threshold, and is rather structureless except for gradual increment from the threshold. It seems also reasonable because of the expected similarities of the structure of the proton states in the isotopes. In Table 3, we summarize the excitation energies E_x , the relative strengths F_R , and the normalization factors $F_O(j_h)$ obtained from the experimental data of the $^{122}\text{Sn}(d,^3\text{He})^{121}\text{In}$ reaction [43], which are used to calculate the quasi-free π^0 production contributions in the $^{122}\text{Sn}(d,^3\text{He})$ reaction.

In Fig. 2, we show the calculated spectra for the formation of the pionic states at finite angles in the $^{117}\text{Sn}(d,^3\text{He})$ and $^{122}\text{Sn}(d,^3\text{He})$ reactions. We find that both spectra have a strong angular dependence because of the matching condition of the reaction by which the different subcomponents dominate the spectra at different angles. We also find that the absolute value of the calculated cross sections in $^{117}\text{Sn}(d,^3\text{He})$ reaction are significantly smaller than that in $^{122}\text{Sn}(d,^3\text{He})$ reaction for all cases considered in this article. In Appendix A, we make some remarks about the difference between the $(d,^3\text{He})$ spectra with ^{117}Sn and ^{122}Sn targets.

4. Conclusion

We study the $(d,^3\text{He})$ reaction for the pionic atom formation on the odd-N nuclear target theoretically. In this reaction, we can expect to observe the pionic states in the even-even nucleus with $J^P = 0^+$. These pionic states populated with the ground state of the daughter nucleus could not be affected by the additional shifts due to the residual interaction effects between the neutron-hole and pionic states. The experimental error of the latest data [5] is significantly smaller than that of the old ones [30, 31] and is now approaching the magnitude of the calculated shifts due to the residual interaction effects [33, 34]. Thus, the observation of the pionic states free from these effects is very important to obtain more accurate information on pion properties in nucleus from the data, which will be necessary to deduce the density dependence of the chiral condensate $\langle \bar{q}q \rangle$ beyond the linear density approximation [35, 36].

We extend the effective number approach to calculate the pionic atom formation spectra on the odd-N nuclear target. In this formulation, we assume that the target nucleus with $J^P = \frac{1}{2}^+$ is composed of the even-even core nucleus with $J^P = 0^+$ and the extra neutron located in the $s_{1/2}$ orbit. Based on this assumption, we consider that the pionic atom in the final state is populated in the even-even core nucleus in the case of single neutron pick-up from the $s_{1/2}$ orbit in the target nucleus in the $(d,^3\text{He})$ reaction. On the other hand, we consider the pionic atoms are populated in the daughter nucleus with the configuration $J = [s_{1/2} \otimes j_h^{-1}]$, where the neutron remaining in the valence $s_{1/2}$ orbit is coupled to a neutron-hole state j_h^{-1} , in the case of neutron pick-up from a single particle orbit j_h other than $s_{1/2}$ in the target. We evaluate separately the effective numbers for these two kinds of final states and obtain the pionic atom formation spectra by summing up all contributions.

In order to predict the realistic spectrum shape of the $(d,^3\text{He})$ reaction, we take into account the normalization factor (F_O) of the neutron state in the target nucleus and the relative strength (F_R) of the nuclear excited levels of the daughter nucleus as in Refs. [27, 41], which are determined using the spectroscopic strength obtained from the experimental data [42].

We show the numerical results of $^{117}\text{Sn}(d,^3\text{He})$ spectra for the pionic atom formation. We find that we can see clearly the peak structure of the pionic $1s$ state formation with the ground state of the daughter nucleus ^{116}Sn which does not have the additional shifts due to the residual interaction effects. By comparing the $^{117}\text{Sn}(d,^3\text{He})$ spectra with those of the $^{122}\text{Sn}(d,^3\text{He})$, we find that the bound pionic state formation spectra in $^{117}\text{Sn}(d,^3\text{He})$ reaction spread over wider energy range than those in $^{122}\text{Sn}(d,^3\text{He})$ reaction because of the larger excitation energies of ^{116}Sn than those of ^{121}Sn . We also find that the absolute values of the calculated cross sections in $^{117}\text{Sn}(d,^3\text{He})$ reaction are significantly smaller than those in $^{122}\text{Sn}(d,^3\text{He})$ reaction because the values of the normalization factor F_O and the relative strength F_R of ^{117}Sn are smaller than those of ^{122}Sn as described in detail in Appendix A.

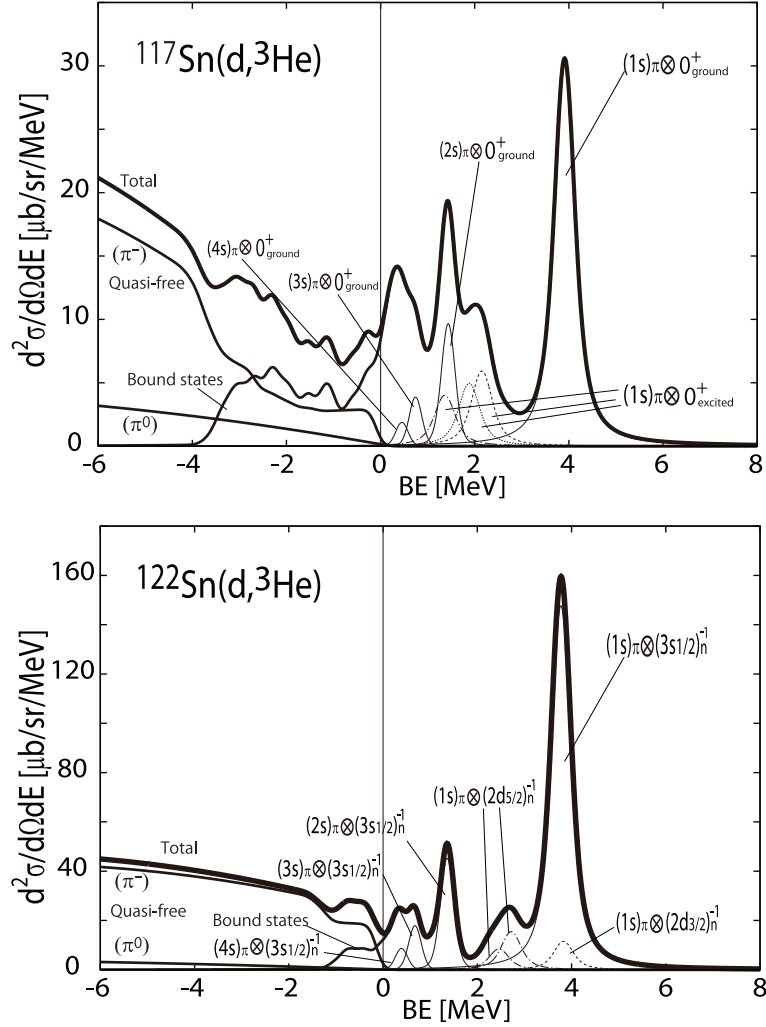


Fig. 1 Calculated spectra for the formation of the pionic states in the $^{117}\text{Sn}(d,^3\text{He})$ (upper) and the $^{122}\text{Sn}(d,^3\text{He})$ (lower) reactions at $\theta_{d\text{He}}^{\text{lab}} = 0^\circ$ plotted as functions of the pion binding energy. The incident deuteron kinetic energy is fixed to be $T_d = 500$ MeV. The total spectra are shown by the thick solid lines in both figures. We show separately the contributions of the bound pionic states formation and the quasi-free π^- and π^0 production by the thin solid lines. The dominant subcomponents are also shown in the figures with quantum numbers indicated as $[(nl)_\pi \otimes J^P]$ in the $^{117}\text{Sn}(d,^3\text{He})$ reaction (upper) and $[(nl)_\pi \otimes (nl_j)_n^{-1}]$ in the $^{122}\text{Sn}(d,^3\text{He})$ reaction (lower), respectively. The instrumental energy resolution is assumed to be 300 keV FWHM. The contribution of the π^0 quasi-free production in the $^{117}\text{Sn}(d,^3\text{He})$ reaction (upper) is assumed to be the same as that of $^{122}\text{Sn}(d,^3\text{He})$ reaction (lower) except for the shift of the threshold energy. See the text for details.

As for the contributions of the subcomponents, we find that the $[(1s)_\pi \otimes 0^+_{\text{ground}}]$ subcomponent dominates the largest peak structure appeared in the spectra around $B.E. \simeq 3.9$ MeV in Fig. 1 in the ^{117}Sn target case, whereas two subcomponents of $[(1s)_\pi \otimes (3s_{1/2})_n^{-1}]$ and $[(1s)_\pi \otimes (2d_{3/2})_n^{-1}]$ are included in ^{122}Sn target case because of the small difference ($\sim 60\text{keV}$) between the separation energies of these two neutron levels in ^{121}Sn [35]. In general, the peak

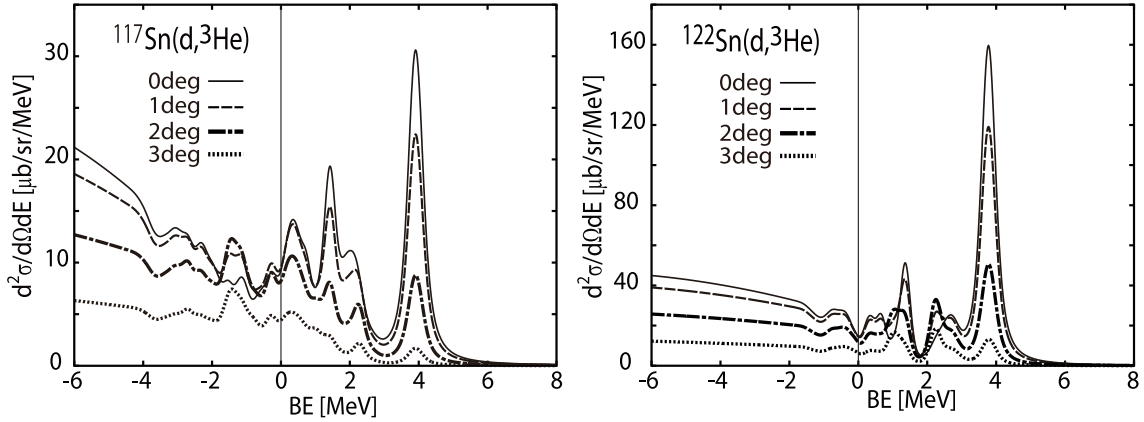


Fig. 2 Calculated spectra for the formation of the pionic states at $\theta_{d\text{He}}^{\text{lab}} = 0^\circ$ (solid lines), 1° (dash lines), 2° (dash-dotted lines) and 3° (dotted lines) in the $^{117}\text{Sn}(d,^3\text{He})$ (left) and the $^{122}\text{Sn}(d,^3\text{He})$ (right) reactions plotted as functions of the pion binding energy. The incident deuteron kinetic energy is fixed to be $T_d = 500$ MeV. The instrumental energy resolution is assumed to be 300 keV FWHM.

in the spectra dominated by a single subcomponent is known to be the most useful to determine the pion binding energy and width because of the absence of the ambiguities in the relative strength of the subcomponents.

In summary, the odd- N nuclear target with $J^P = \frac{1}{2}^+$ is expected to be suited for the pionic $1s$ state observation because the calculated spectra for ^{117}Sn target clearly show the isolated peak structure of the pionic $1s$ state formation with the ground state of the even-even nucleus ($[(1s)_\pi \otimes 0_{\text{ground}}^+]$), having no residual interaction effects.

Thus, the formation of the pionic $1s$ state by the $(d,^3\text{He})$ reactions on the odd- N nuclear target is preferable to extract the most accurate information on the parameter of the QCD symmetry from the observation. However, we need to be careful for the absolute values of the cross sections for the ^{117}Sn target case, which are expected to be smaller than those of ^{122}Sn target.

The experiment for the pionic atom formation on the odd- N nuclear target will be performed at RIBF/RIKEN in near future [44]. We think that these studies will provide the systematic information on the pionic bound states in various nuclei and will help to develop the study of the pion properties and the partial restoration of chiral symmetry in nuclei. We believe that our results provide a good motivation for further experimental studies.

Acknowledgment

We acknowledge the fruitful discussions from the experimental side with K. Itahashi, T. Nishi and H. Fujioka. We thank H. Nakada for the useful comments on the structure of the ground state of the odd-neutron nucleus. We also thank D. Jido for the useful discussions. N. I. appreciates the support by the Grant-in-Aid for JSPS Fellows (No. 23-2274). This work is partly supported by the Grants-in-Aid for Scientific Research (No. 24105707 and No. 24540274).

References

- [1] K. Yagi, T. Hatsuda and Y. Miake, Quark-Gluon Plasma, Cambridge Univ. Press (Cambridge, 2005).
- [2] T. Hatsuda and T. Kunihiro, Phys. Rept. **247**, 221 (1994), and references therein.
- [3] E. Friedman and A. Gal, Phys. Rep. **452**, 89 (2007).
- [4] T. Yamazaki, S. Hirenzaki, R.S. Hayano, H. Toki, Phys. Rep. **514**, 1 (2012).
- [5] K. Suzuki *et al.*, Phys. Rev. Lett. **92**, 072302 (2004).
- [6] E. E. Kolomeitsev, N. Kaiser and W. Weise, Phys. Rev. Lett. **90**, 092501 (2003).
- [7] D. Jido, T. Hatsuda and T. Kunihiro, Phys. Lett. **B670**, 109 (2008).
- [8] H. Nagahiro and S. Hirenzaki, Phys. Rev. Lett. **94**, 232503 (2005).
- [9] H. Nagahiro, M. Takizawa, and S. Hirenzaki, Phys. Rev. **C74**, 045203 (2006).
- [10] D. Jido, H. Nagahiro, S. Hirenzaki, Phys. Rev. **C 85 (R)**, 032201 (2012).
- [11] H. Nagahiro, S. Hirenzaki, E. Oset, A. Ramos, Phys. Lett. **B 709**, 87 (2012).
- [12] K. Itahashi *et al.*, Prog. Theor. Phys. **128**, 601 (2012).
- [13] T. Kishimoto, Phys. Rev. Lett. **83**, 4701 (1999).
- [14] S. Hirenzaki, Y. Okumura, H. Toki, E. Oset, and A. Ramos, Phys. Rev. **C61**, 055205 (2000).
- [15] K. Ikuta, M. Arima, and K. Masutani, Prog. Theor. Phys. **108**, 917 (2002).
- [16] J. Yamagata, H. Nagahiro, Y. Okumura, and S. Hirenzaki, Prog. Theor. Phys. **114**, 301 (2005) [Errata-*ibid* **114**, 905 (2005)].
- [17] J. Yamagata, H. Nagahiro, and S. Hirenzaki, Phys. Rev. **C74**, 014604 (2006).
- [18] Q. Haider and L. C. Liu, Phys. Lett. **B172**, 257 (1986).
- [19] R. S. Hayano, S. Hirenzaki, and A. Gillitzer, Eur. Phys. J. A **6**, 99 (1999).
- [20] D. Jido, H. Nagahiro, and S. Hirenzaki, Phys. Rev. **C66**, 045202 (2002).
- [21] H. Nagahiro, D. Jido, and S. Hirenzaki, Phys. Rev. **C68**, 035205 (2003).
- [22] D. Jido, E. E. Kolomeitsev, H. Nagahiro, and S. Hirenzaki, Nucl. Phys. **A811**, 158 (2008).
- [23] H. Toki and T. Yamazaki, Phys. Lett. **B213**, 129 (1988).
- [24] H. Toki, S. Hirenzaki, T. Yamazaki and R.S. Hayano, Nucl. Phys. **A501**, 653 (1989).
- [25] H. Toki, S. Hirenzaki and T. Yamazaki, Nucl. Phys. **A530**, 679 (1991).
- [26] S. Hirenzaki, H. Toki and T. Yamazaki, Phys. Rev. **C44**, 2472 (1991).
- [27] Y. Umemoto, S. Hirenzaki, K. Kume and H. Toki, Phys. Rev. **C62**, 024606 (2000).
- [28] T. Yamazaki *et al.*, Z. Phys. **A355**, 219 (1996).
- [29] H. Gilg *et al.*, Phys. Rev. **C62**, 025201 (2000).
- [30] K. Itahashi *et al.*, Phys. Rev. **C62**, 025202 (2000).
- [31] H. Geissel *et al.*, Phys. Rev. Lett. **88**, 122301 (2002).
- [32] K. Itahashi *et al.*, Proceedings of the 20th International IUPAP Conference on Few-Body Problems in Physics (FB20), submitted to Few-Body Systems;
S. Itoh, “Precision spectroscopy of deeply bound states in the pionic ^{121}Sn atom”, Doctor Thesis, University of Tokyo, December (2011).
- [33] S. Hirenzaki, H. Kaneyasu, K. Kume, H. Toki, Y. Umemoto, Phys. Rev. **C60**, 058202 (1999).
- [34] N. Nose-Togawa, H. Nagahiro, S. Hirenzaki and K. Kume, Phys. Rev. **C71**, 061601(R) (2005).
- [35] N. Ikeno, R. Kimura, J. Yamagata-Sekihara, H. Nagahiro, D. Jido, K. Itahashi, L.S. Geng, S. Hirenzaki, Prog. Theor. Phys. **126**, 483 (2011).
- [36] S. Goda and D. Jido, EPJ Web of Conferences **37**, 08010 (2012).
- [37] N. Ikeno, H. Nagahiro and S. Hirenzaki, Eur. Phys. J. A **47**, 161 (2011).
- [38] H. Koura and M. Yamada, Nucl. Phys. **A671**, 96 (2000).
- [39] M. Betigeri *et al.*, Nucl. Phys. **A690**, 473 (2001).
- [40] S. Hirenzaki, H. Toki, Nucl. Phys. **A 628**, 403 (1998).
- [41] Y. Umemoto, S. Hirenzaki and K. Kume, Prog. Theor. Phys. **103**, 337 (2000).
- [42] J.M. Schippers *et al.*, Nucl. Phys. **A510**, 70 (1990).
- [43] C.V. Weiffenbach and R. Tickle, Phys. Rev. **C3**, 1668 (1971).
- [44] K. Itahashi *et al.*, ‘Precision Spectroscopy of Pionic Atoms in ($d,^3\text{He}$) Nuclear Reactions’: Exp. proposal NP0702-RIBF-027 for RIBF, December (2006); ‘Spectroscopy of Pionic Atom in $^{122}\text{Sn}(d,^3\text{He})$ Nuclear Reaction’: Exp. proposal NP0802-RIBF-054 for RIBF, January (2008).

A. Comparison of the ($d,^3\text{He}$) spectra of the pionic atom formation on the ^{117}Sn and ^{122}Sn targets

In this appendix, we discuss the origin of the differences of the calculated cross sections of the pionic atom formation in the ($d,^3\text{He}$) reaction on the ^{117}Sn and ^{122}Sn target cases. As shown

Table A1 Symbols used in this Appendix and definitions of the effective number (N_{eff}), the normalization factor (F_O), and the relative strength (F_R) are summarized for the odd- and even-neutron nuclear target cases. As for the odd-N nuclear target with $J^P = \frac{1}{2}^+$, we distinguish two cases of the final state of the ($d, {}^3\text{He}$) reaction and treat them separately. See details in the text.

Target nucleus	Odd nucleus with $J^P = \frac{1}{2}^+$ (ex. ${}^{117}\text{Sn}$)		Even nucleus (ex. ${}^{122}\text{Sn}$)
Neutron state in target	$s_{1/2}$	j_h	j_h
Spin of daughter nucleus	0	$[s_{1/2} \otimes j_h^{-1}]_J$	j_h^{-1}
Effective number (N_{eff})	$N_{\text{eff}}^{\text{odd}(1)}(\ell_\pi \otimes (J^P = 0^+))$ (Eq. (3))	$N_{\text{eff}}^{\text{odd}(2)}(\ell_\pi \otimes [s_{1/2} \otimes j_h^{-1}]_J)$ (Eq. (4))	$N_{\text{eff}}^{\text{even}}(\ell_\pi \otimes j_h^{-1})$
Normalization factor (F_O)	$F_O^{\text{odd}}(s_{1/2})$ (Eq. (16))	$F_O^{\text{odd}}(j_h)$ (Eq. (15))	$F_O^{\text{even}}(j_h)$
Relative strength (F_R)	$F_R^{\text{odd}}((J^P = 0^+)_N)$ (Eq. (18))	$F_R^{\text{odd}}([s_{1/2} \otimes j_h^{-1}]_J)_N)$ (Eq. (17))	$F_R^{\text{even}}((j_h^{-1})_N)$

in Fig. 1, the cross section of ${}^{117}\text{Sn}(d, {}^3\text{He})$ is about one over five of that of ${}^{122}\text{Sn}(d, {}^3\text{He})$ at the largest peak position at $B.E. \simeq 3.9$ MeV. We think that this difference is large even if we take into account the fact that the spectra of one-neutron pick-up process from ${}^{117}\text{Sn}$ spread over wider energy region than those from ${}^{122}\text{Sn}$ due to the larger excitation energies of the daughter nucleus as shown in Table 2.

In the effective number approach used to evaluate the pionic atom formation cross section in this article, the size of the formation cross section of the pionic states is described by the effective number N_{eff} defined in Eqs. (3) and (4), and the additional factors F_O and F_R introduced in Eqs. (13) and (14). Thus, we discuss the difference of these parts separately.

In Table A1, we first summarize the symbols used in this Appendix and definitions of the effective number (N_{eff}), the normalization factor (F_O) and the relative strength (F_R) for the odd-neutron (odd-N) and even-neutron (even-N) nuclear target cases. As for the odd-N nuclear target with $J^P = \frac{1}{2}^+$, we distinguish two cases of the final state of the ($d, {}^3\text{He}$) reaction and treat them separately as shown in Eq. (2) in Section 2. In the case of neutron pick-up from the $s_{1/2}$ orbit in the target nucleus, the pionic atoms are populated in the even-even core nucleus with $J^P = 0^+$. We express in this case the effective number as $N_{\text{eff}}^{\text{odd}(1)}(\ell_\pi \otimes (J^P = 0^+))$, the normalization factor as $F_O^{\text{odd}}(s_{1/2})$, and the relative strength as $F_R^{\text{odd}}((J^P = 0^+)_N)$, which are defined by Eqs. (3), (16) and (18), respectively. In the case of neutron pick-up from a single particle orbit j_h other than $s_{1/2}$ in the target, the pionic atoms are populated in the nucleus with the configuration $J = [s_{1/2} \otimes j_h^{-1}]$, where the neutron remaining in the valence $s_{1/2}$ orbit is coupled to the neutron-hole state j_h^{-1} to form the total nuclear spin J . We express in this case the effective number as $N_{\text{eff}}^{\text{odd}(2)}(\ell_\pi \otimes [s_{1/2} \otimes j_h^{-1}]_J)$, the normalization factor as $F_O^{\text{odd}}(j_h)$, and the relative strength as $F_R^{\text{odd}}([s_{1/2} \otimes j_h^{-1}]_J)_N)$, which are defined by Eqs. (4), (15) and (17), respectively. As for the even-N nuclear target case, the pionic atoms are populated in the nucleus with a neutron-hole state j_h^{-1} . The effective number $N_{\text{eff}}^{\text{even}}(\ell_\pi \otimes$

j_h^{-1}), the normalization factor as $F_O^{\text{even}}(j_h)$, and the relative strength as $F_R^{\text{even}}((j_h^{-1})_N)$ for the even-N nuclear target case are defined in Refs. [27, 35, 41].

In the considerations below, we postulate that the differences of the wave functions and distortion factors between ^{117}Sn and ^{122}Sn targets are small and can be neglected safely. In this case, it is known that the relative size of the effective numbers are determined by the multiplicity of the states and satisfy the relation, for example,

$$N_{\text{eff}}^{\text{odd}(2)}(\ell_\pi \otimes [s_{1/2} \otimes j_h^{-1}]_{J_1}) : N_{\text{eff}}^{\text{odd}(2)}(\ell_\pi \otimes [s_{1/2} \otimes j_h^{-1}]_{J_2}) = (2J_1 + 1) : (2J_2 + 1). \quad (\text{A1})$$

We consider first the pionic atom formation in the case with a neutron picked-up from the $s_{1/2}$ orbit in the target nucleus. For the odd-N nuclear ^{117}Sn target case, the effective number for the pionic atom (ℓ_π) formation in the even-even core nucleus ($J^P = 0^+$) is written as $N_{\text{eff}}^{\text{odd}(1)}(\ell_\pi \otimes (J^P = 0^+))$ as shown in Table A1. For the even-N nuclear ^{122}Sn target case, the pionic atoms are populated in the nucleus with a neutron-hole state $s_{1/2}^{-1}$, and the effective number is written as $N_{\text{eff}}^{\text{even}}(\ell_\pi \otimes s_{1/2}^{-1})$. By comparing the formula of these effective numbers, we found the following relation,

$$N_{\text{eff}}^{\text{even}}(\ell_\pi \otimes s_{1/2}^{-1}) = 2N_{\text{eff}}^{\text{odd}(1)}(\ell_\pi \otimes (J^P = 0^+)). \quad (\text{A2})$$

The effective number of the even-N nuclear target is twice larger than that of the odd-N nuclear target. This is simply because that we assumed the number of neutron in the fully occupied $s_{1/2}$ orbit in ^{117}Sn is equal to be 1 in the effective number formalism in Section 2 as explained in Eq. (1). Therefore, in this case, we found that the cross section on the odd-N nuclear target is half of that on the even-N nuclear target.

Then, we consider the pionic atom formation in the case of neutron pick-up from single particle orbits other than $s_{1/2}$ in the target. For the odd-N nuclear ^{117}Sn target case, the pionic atoms are populated in the nucleus with the configuration $J = [s_{1/2} \otimes j_h^{-1}]$, where the neutron remaining in the valence $s_{1/2}$ state couples to a neutron-hole state j_h^{-1} to form the total nuclear spin J which can take two values as $J_1 = j_h - \frac{1}{2}$ and $J_2 = j_h + \frac{1}{2}$. The effective numbers for the pionic state (ℓ_π) formation in the daughter nucleus with the spin $J = J_1, J_2$ are written as $N_{\text{eff}}^{\text{odd}(2)}(\ell_\pi \otimes [s_{1/2} \otimes j_h^{-1}]_{J_1})$ and $N_{\text{eff}}^{\text{odd}(2)}(\ell_\pi \otimes [s_{1/2} \otimes j_h^{-1}]_{J_2})$, respectively. For the even-N nuclear ^{122}Sn target case, the pionic atoms are populated in the nucleus with a neutron-hole state j_h^{-1} and the effective number is written as $N_{\text{eff}}^{\text{even}}(\ell_\pi \otimes j_h^{-1})$. In this case, we found another relation written as,

$$N_{\text{eff}}^{\text{even}}(\ell_\pi \otimes j_h^{-1}) = N_{\text{eff}}^{\text{odd}(2)}(\ell_\pi \otimes [s_{1/2} \otimes j_h^{-1}]_{J_1}) + N_{\text{eff}}^{\text{odd}(2)}(\ell_\pi \otimes [s_{1/2} \otimes j_h^{-1}]_{J_2}), \quad (\text{A3})$$

between the effective numbers for the pionic atom formation by the ($d, ^3\text{He}$) reactions on the even-N and odd-N nuclear targets. This relation means that the effective number of the even-N nuclear target is equal to the sum of the effective numbers of the odd-N nuclear target for the same combination of ℓ_π and j_h^{-1} . Therefore, in this case, we found that the ($d, ^3\text{He}$) total cross section obtained by summing up the all subcomponents should take similar values both for even-N and odd-N nuclear target cases.

Hence, as for the effective numbers, we do not find the origin of the significant differences of the absolute value of the ($d, ^3\text{He}$) total cross sections on the even-N and odd-N nuclear target cases as shown in Eq. (A3), except for the factor 2 difference of the contribution from the $s_{1/2}$ neutron as shown in Eq. (A2).

Finally, we consider the effects of the additional factors F_O and F_R introduced in Eqs. (13) and (14). To clarify the effects, we investigate the height of the largest peak structure appeared in the spectra around $B.E. \simeq 3.9$ MeV in Fig. 1 as an example and evaluate the effects of the F_O and F_R factors. The largest peak mainly consists of the contributions of the neutron pick-up from the $s_{1/2}$ state for both ^{122}Sn and ^{117}Sn target cases. We pay special attention to the dominant subcomponent $[(1s)_\pi \otimes 0_{\text{ground}}^+]$ for ^{117}Sn target and the $[(1s)_\pi \otimes (3s_{1/2})_n^{-1}]$ for ^{122}Sn target. According to Eq. (A2), the effective numbers of these subcomponents satisfy the relation,

$$\frac{N_{\text{eff}}^{\text{odd}(1)}([(1s)_\pi \otimes 0_{\text{ground}}^+])}{N_{\text{eff}}^{\text{even}}([(1s)_\pi \otimes (3s_{1/2})_n^{-1}])} = \frac{1}{2}. \quad (\text{A4})$$

We consider the effects of the F_O and F_R factors to this ratio. From Eq. (13), the ratio is modified by including F_O and F_R as,

$$\frac{N_{\text{eff}}^{\text{odd}(1)}([(1s)_\pi \otimes 0_{\text{ground}}^+]) \times F_O^{\text{odd}} \times F_R^{\text{odd}}}{N_{\text{eff}}^{\text{even}}([(1s)_\pi \otimes (3s_{1/2})_n^{-1}]) \times F_O^{\text{even}} \times F_R^{\text{even}}} = \frac{1 \times 0.47 \times 0.68}{2 \times 0.7 \times 1} \simeq \frac{1}{4}, \quad (\text{A5})$$

where the F_O and F_R factors for ^{117}Sn are $F_O^{\text{odd}} = 0.47$ and $F_R^{\text{odd}} = 0.68$ as listed in Tables 1 and 2, and for ^{122}Sn they are $F_O^{\text{even}} = 0.7$ and $F_R^{\text{even}} = 1$ as reported in Tables V and VI of Ref. [35]. By including F_O and F_R , the height of the largest peak of the spectra of the ^{117}Sn target is reduced to around 32% ($= 0.47 \times 0.68$) of its original value due to the effects of both factors. On the other hand, as for the ^{122}Sn target case, the height is reduced to around 70% due to the effect of F_O . The F_R factor of ^{122}Sn is equal to 1 and do not change the height of the peak. Consequently, we found that the height of the largest peak structure of the ^{122}Sn target is expected to be about four times larger than that of the ^{117}Sn target by including the F_O and F_R factors as shown in Eq. (A5). We think this is the reason why the cross sections in Fig. 1 show the differences between ^{122}Sn and ^{117}Sn targets. We should notice here that the effect of F_R is just to split one peak into several small peaks corresponding to the plural nuclear excitations with the same quantum numbers. Thus, the energy integrated total cross section is hardly changed by the F_R factor.

We conclude that the origins of the difference of the absolute value of the cross sections on the ^{117}Sn and ^{122}Sn targets are the factor two difference of the effective numbers N_{eff} of the $s_{1/2}$ neutron pick-up process, and the values of the F_O and F_R factors which reflect the occupation probability of the neutron states in the target and the relative strength of the excited levels of the daughter nucleus. Here, we should be careful on the differences of the effects of F_O and F_R . The effect of F_O makes the height of the peak lower and also makes the energy integrated total cross section smaller, whereas F_R only divides the peak into small peaks and spreads in the energy spectrum. Hence, the value of the energy integrated total cross section changes little even if the F_R factor is taken into account.